Environmental Science
Processes & Impacts

Accepted Manuscript

Environmental impact statement

The accident of TEPCO's Fukushima Daiichi Nuclear Power Plant released large amounts of radionuclides, especially radiocesium, to the environment and has still been affecting residents in the vicinity of the plant. However, little measurement data associated with contaminated seabed sediments at Fukushima has been published in open literature. Since the accident-derived radiocesium in seabed sediments are expected to remain over a decadal scale, continuous monitoring and accurate prediction are highly recommended. In this paper, the distributional pattern of the initial deposition of radiocesium in the surrounding regions of the plant is outlined, and primary processes accumulating radiocesium in the seabed are assessed based on the inventory data. This paper provides helpful information in planning of effective monitoring as well as in estimation of the impact of the accident on the marine ecosystem.

Table of contents entry

About seven months after the accident in Fukushima, approximately 0.2 PBq of ^{134}Cs was accumulated in seabed sediment.

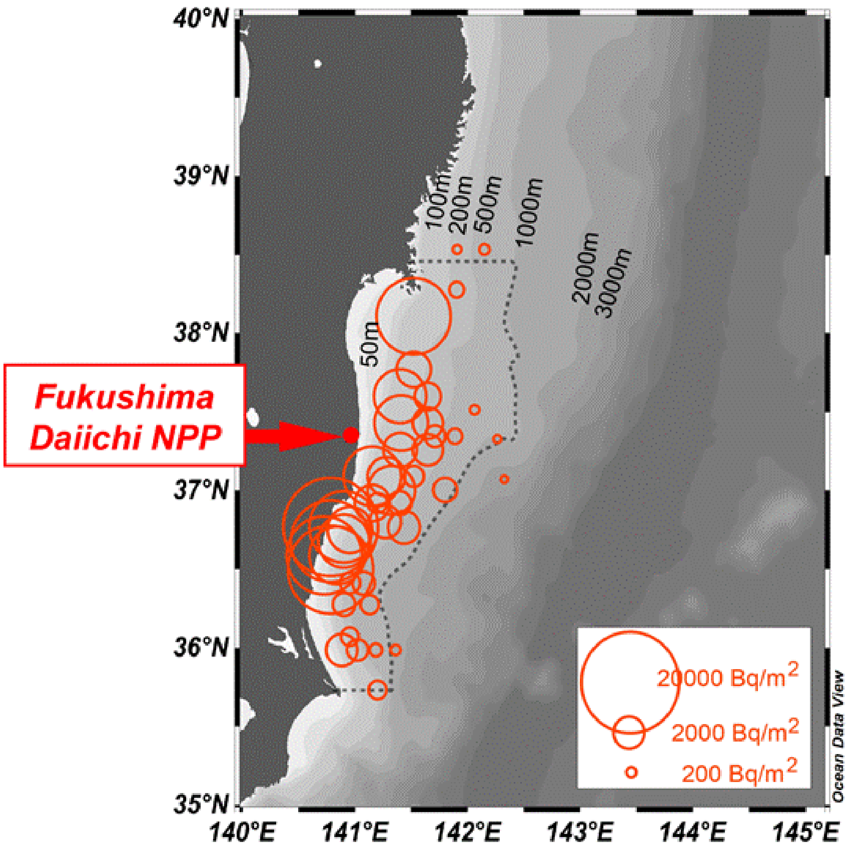

Radiocesium derived from the Fukushima Daiichi Nuclear Power Plant accident in seabed sediments: Initial deposition and inventories.

Shigeyoshi Otosaka[1,*], Yoshihisa Kato[2]

[1]*Research Group for Environmental Sciences, Japan Atomic Energy Agency, Tokai-mura, Ibaraki 319-1195, Japan*

[2]*School of Marine Science and Technology, Tokai University, Shimizu-ku, Shizuoka 424-8610, Japan*

*Corresponding author:

Phone +81.29.282.5171; Facsimile +81.29.282.6760; E-mail otosaka.shigeyoshi@jaea.go.jp

Abstract

Since the accident of Fukushima Dai-ichi Nuclear Power Plant (1FNPP), significant levels of anthropogenic radionuclides have been detected from seabed sediments off the east coast of Japan. In this paper, the approximate amount of accident-derived radiocesium in seabed sediments off Fukushima, Miyagi and Ibaraki prefectures was estimated from a sediment integration algorithm. As of October 2011, about half year after the accident, the total amount of sedimentary ^{134}Cs was 0.20±0.06 PBq (decay corrected to March 11, 2011) and more than 90% of the radiocesium was accumulated in the regions shallower than 200 m depths. The large inventory in the coastal sediments was attributed to effective adsorption of dissolved radiocesium onto suspended particles and directly to sediments in the early post-accidental stage. Although rivers are also an important source to supply radiocesium to the coastal regions, this flux was much lower than that of the above-mentioned process within half a year after the accident.

1. Introduction

On March 11, 2011, the Great East Japan Earthquake and the associated tsunami triggered the TEPCO's Fukushima Daiichi Nuclear Power Plant (1FNPP) accident. The accident released large amounts of radionuclides to the environment and has still been affecting residents in the vicinity of the plant. Monitoring surveys of the marine environment in the early post-accident stage detected significant levels of radionuclides from seawater and seabed sediments collected at 30~180 km from 1FNPP.[1] Among the radionuclides, two radioisotopes of cesium; ^{134}Cs and ^{137}Cs, have been major radionuclides that should be monitored from a viewpoint of radiological dose assessment. While concentrations of radiocesium in nearshore seawater decreased by two orders of magnitude within a year after the accident,[2,3,4] those in seabed sediments have not decreased remarkably.[5,6]

Two major mechanisms are known to affect the concentration of cesium in seabed sediments. One is the electrostatically-controlled adsorption of cesium ions (Cs^+) onto the surface of clay minerals[7] or within the interlayer which leads to inner sphere complexes.[8] This mechanism occurs by contact of Cs^+ with clay minerals. The second mechanism is the biological uptake of Cs^+ into organisms and their subsequent settling to the seabed.[9-11] Otosaka and Kobayashi[6] found that most of the accident-derived associated with seabed sediments, and the characteristics are consistent with the low mobility of sedimentary radiocesium. It is also indicated that the low mobility of sedimentary radiocesium correlates with elevated concentrations of radiocesium in bottom-dwelling fishes near Fukushima.[12-15]

Since the accident-derived radiocesium in seabed sediments are thus expected to remain over a decadal scale, continuous monitoring and accurate prediction are highly recommended. As the first step, it is necessary to explain processes controlling the initial distribution of the radiocesium in seabed sediment and the amount of the initial deposition. In order to estimate the inventory of sedimentary radiocesium, concentrations of the radiocesium as well as the thickness that radiocesium penetrates into the sediment needs to be understood. The upper 0-3 cm of seabed sediment is regarded as a reference layer to assess radiological effects on the benthic ecosystem.[16] Since the 1FNPP accident, much monitoring data of sedimentary radiocesium have actually been obtained from this layer.[5] These data are helpful to observe the general distribution of radionuclides in the reference layer, but are sometimes inadequate to estimate the amount of radionuclides in the sediment because a significant amount of radiocesium penetrates to the deeper sedimentary layers. In this paper, an index to associate monitoring data with inventory of sedimentary radiocesium is proposed, and the distributional pattern of the initial deposition of radiocesium in the surrounding regions of 1FNPP is outlined. In addition, primary processes accumulating radiocesium in the seabed are assessed based on the inventory data.

2. Methods

2.1 Data sources

Cumulative inventories of radiocesium in seabed sediment were estimated from observation data obtained at 44 stations (Table 1 and Fig. 1). The data consist of three datasets. Data from 13 stations categorized as “A” in Table 1 were obtained by two sampling campaigns in August 2011 and October/November 2011 (see subsection 2.2 for details). Since this dataset contains data obtained from broad area of the study area (depth range: 105~1175 m) for 0~10 cm of sedimentary layers, and covers the lack of monitoring data (category “C” data described below) for sedimentary layers below 3 cm. Seabed sediments in the nearshore region (< 100 m depth) consist of coarse and fine sand.[17] Because it is quite difficult to observe accurate vertical profiles of the radionuclides in such sandy sediment, data on the cumulative inventory of the radionuclides are quite limited. In this paper, we regarded cumulative inventories obtained at seven coastal stations 70~110 km south from 1FNPP [6] as representative ones of coastal regions (category “B” in Table 1). Data from the other 24 stations, categorized “C”, were obtained from monitoring program by the Ministry of Education, Culture, Sports, Science and Technology, Japan and compiled by Kusakabe et al.[5] The category “C” dataset provides data only for upper 3 cm of the sediment. Calculations of cumulative inventories of radiocesium are different for each data source.

2.2 Sampling

Sediment samples with category “A” stations were collected in R/V Tansei-Maru KT-11-27 cruise (October-November 2011) and R/V Hakuho-Maru KH-11-07 cruise (August 2011) using a multiple corer. Core samples (80 mm in diameter) were subsampled by cutting into 1 cm thickness sections on board the ship and transferred to laboratories on land for the further processes.

2.3 Analysis of radiocesium and sediment properties

After being transferred to the laboratory on land, sediment samples were dried at 105°C, crushed, and the coarse fractions were removed using a 2 mm sieve.[16] Powdered sediment samples were filled and sealed in a plastic container.

Specific gamma-rays of ^{134}Cs (604 and 795 keV) and ^{137}Cs (661 keV) were measured using a coaxial Ge detector (ORTEC GEM20P4, 1.7 keV/1.33 MeV of resolution and 29~31% of relative efficiencies). The ^{134}Cs/^{137}Cs counting ratio with the least contribution from summing effects was estimated by measurement of a soil sample collected in Fukushima after the FDNPP accident at a distance (~20 cm) from the detector. By comparing this ratio with that measured under the same conditions for the sample in contact with the detector, the contribution due to cascade summing of ^{134}Cs was then estimated for each detectors used in this study, and corrected for all samples. Specific gamma-rays of ^{210}Pb (46.5 keV) and ^{214}Pb (352 keV) were measured using a low-energy photon detector (ORTEC LOAx-51370/20P, 625 keV/122 keV of resolution). Activities of the excess-^{210}Pb ($^{210}Pb_{xs}$) were calculated by subtracting ^{214}Pb activities from the ^{210}Pb activities on the assumption that the supported ^{210}Pb from ^{226}Ra is equal to ^{214}Pb. Gamma detectors were calibrated using standard material (MX033U8PP, Japan Radioisotope Association, Tokyo). Under our analytical conditions (36,000~200,000 seconds counting), the lowest amount of ^{134}Cs and ^{137}Cs that could be determined in a sediment sample was ~87 mBq and ~73 mBq, corresponding to ~5 Bq/kg and ~4 Bq/kg, respectively.

Concentrations of radiocesium reported in the following sections are represented as Bq/kg by dry weight. For all sediment samples, water content and dry bulk density were measured with a given volume of plastic tube. The organic matter content was determined by the loss of ignition method: the samples were heated in a muffle furnace at 500°C for 24 hours. Size distribution of sediment was measured using a laser diffraction particle size analyzer (Shimadzu SALD-2000J).

2.4 Data analysis

Since it is estimated that ^{137}Cs was also discharged to the ocean by the 1FNPP accident with a uniform ^{134}Cs/^{137}Cs activity ratio (0.99±0.03, as of March 11, 2011),[2] both ^{134}Cs and ^{137}Cs should be concerned. Both radionuclides had been released to the environment by nuclear weapon testing, operation of spent nuclear fuel reprocessing plants or accidents of nuclear facilities.[18-20] At the time of the outbreak of 1FNPP accident, slightly but significant amount of ^{137}Cs (half-live: 30.1 years) originates from such past incidents remained in seabed sediments near Fukushima, and ^{134}Cs (half-live: 2.06 years) was undetectable.[5] In order to estimate the amount of radiocesium derived from the 1FNPP accident in the seabed sediment, we report data of ^{134}Cs as representative radiocesium with few influence of the other sources.

With regard to category "A" stations, inventory of sedimentary radiocesium in each sub-sample was calculated by multiplying the radiocesium concentration with the bulk density (see Appendix). By cumulating the radiocesium inventories to 10 cm layer, cumulative inventory of sedimentary radiocesium at each station was estimated. Based on the inventory data, $F_{0\text{-}3}$ values, defined as the proportion of ^{134}Cs inventory in the upper 3 cm to the cumulative inventory in the sediment core, were estimated.

In this paper, activities data were normalized (decay-corrected) to March 11, 2011 to estimate the total amount of sedimentary radiocesium from various data sources.

3. Results and discussion

3.1 Vertical distribution of radiocesium in sediment

Vertical changes in ^{134}Cs concentration and sediment properties (bulk density, $^{210}Pb_{xs}$, and organic matter content) at three representative stations (J7, J8 and FS1) are shown in Fig. 2 (a)~(c). Three patterns of the ^{134}Cs profile were found in this study, and the lateral distribution of the three patterns is shown in Fig. 2 (d).

Sediment at Sta. J7 mainly consisted of sand (Table 1). A discontinuous surface of $^{210}Pb_{xs}$ was found at 3-4 cm layer (indicated "A" in Fig. 2(a)), and slightly lower content of manganese indicated reductive characteristics of the layer. The ^{134}Cs concentrations in sediment decreased exponentially with increasing depth, and most of ^{134}Cs was accumulated between the surface and the boundary layer. Sediments characterized by such profiles (categorized as Pattern I) distributed over a wide area of this study (Fig. 2(d)). It can be considered that the boundary layer was formed by the earthquake and the following tsunami in March 2011, and accident-radiocesium was permeated into the upper layers of the boundary.

In Sta J8, at least two boundaries were found and significant ^{134}Cs concentrations were distributed across the boundaries (Fig. 2(b)). This characteristics of ^{134}Cs profile, categorized as "Pattern II", was observed at stations located the south of 1FNPP (Fig. 2(d)). A significant accumulation of anthropogenic heavy metals, such as zinc, was observed near the lower boundary layer (indicated "C" in Fig. 2(b)). It is likely that the "C" layer is also attributable to the earthquake and tsunami, and ^{134}Cs was diffused to the deeper layers of the sediment in the early post-accident stage. Large earthquake and the following tsunami caused high turbulence in the water on the seafloor. The median diameter of surface sediment at this station was 40 μm. Even if we assume a calm condition (slowest sinking) and general hydrographical parameters,[21] estimated sinking rates would be in the order of 10^{-4} m/s. Therefore, if the fine particles were resuspended in the bottom waters, it would take several days to weeks to resettle to the seabed. This timescale is sufficient for the accident-derived radionuclides to adsorb onto the suspended particles in the water column.

In Sta. FS1, no disturbance of the sedimentary layer was observed (Pattern III). Such a characteristic was found in the offshore regions, and all of ^{134}Cs was accumulated in the upper 3 cm layers (Fig. 2(c)). In the offshore stations, ^{134}Cs would be supplied into the sedimentary layers across the sediment-water interface and diffused to the deeper layers of the sediment.

In this study, almost all of the accident-derived radiocesium was observed in the layers upper 10 cm. Although significant concentrations of ^{134}Cs were detected at 10 cm layers at Sta. K2, the proportion of ^{134}Cs below the 10 cm layers is expected to less than 5% of the total ^{134}Cs inventory in the station. In the following subsections, we estimate a total amount of ^{134}Cs in sediment by integrating ^{134}Cs inventory from the surface to 10 cm layers.

Relationship between $F_{0\text{-}3}$ values and bottom depth is shown in Fig. 3. The $F_{0\text{-}3}$ values were less than 0.5 in the nearshore regions (<100 m depth), indicating that more than half of the radiocesium was accumulated into sedimentary layer deeper than 3 cm.

$F_{0\text{-}3}$ values in the offshore (water depth: 100~400 m) and hemiplegic (>400m) regions ranged 0.78±0.16 and 0.93±0.14, respectively. Although the $F_{0\text{-}3}$ values generally increased toward offshore regions, a proportion of radiocesium was accumulated in the deeper layers of sediment. It is difficult to simplify $F_{0\text{-}3}$ values with a specific parameter because the value is controlled by various factors such as bulk density of sediment, radiocesium concentration in the bottom water, bottom current, and bioturbation. As mentioned above, the F_{0-3} values are also affected by sedimentary processes attributable to the earthquake and tsunami. Nevertheless, at least for the nearshore and offshore regions in this study area, results in Fig. 3 indicate that representative F_{0-3} values can be applied to obtain an inventory of sedimentary radiocesium.

3.2 Lateral distribution of radiocesium inventory in seabed sediment

Estimated ^{134}Cs inventories in the seabed sediment observed in October and November 2011 are shown in Table 1 and Fig. 4. As described in the subsection 2.2, data shown in this figure consists of three groups. Within the three groups, data from Otosaka and Kobayashi,[6] categorized as “B” in Table 1, are ^{134}Cs inventories accumulated to the 10 cm sedimentary layer. Since radiocesium penetrates to more than 10 cm depths in the nearshore sediments, these data might be an underestimate of the “total” inventories. Data obtained from 24 stations, categorized as “C” in Table 1, are estimated with the following equation (1).

$$I = C_{0-3} \times \delta / F_{0-3}\,, \qquad (1)$$

where, I is the cumulative ^{134}Cs inventory in sediment (Bq/m^2), C_{0-3} is the ^{134}Cs concentration in upper 3 cm layer (Bq/kg), and δ is the dry bulk density (kg/L).[5] As shown in Fig. 3, radiocesium permeates into the deeper layers of the coastal sediment, and this enhances uncertainty of F_{0-3} values. We thus did not include monitoring data at the nearshore (<100 m) stations in the category “C” dataset although much data had been obtained from the coastal region.[5]

As uncertainty of F_{0-3} values is determined as the 95% confident interval, uncertainties of ^{134}Cs inventory for category “C” data propagate to ±30%. Uncertainties of cumulative ^{134}Cs inventory for “A” and “B” categories, less than ±10%, are smaller than those of category “C” data. Although it would be inappropriate to summarize datasets with different data qualities, all data are summarized in Fig. 4 in order to overview the distribution of ^{134}Cs inventories in the study area.

Fig. 4 clearly shows that inventories of ^{134}Cs are remarkably higher in the coastal and nearshore regions at the latitudinal range between 35°40’ N and 38°30’ N. In this region, the Tsugaru Warm Current flows southward and the Kuroshio Current flows northward along the coast.[22,23] Both currents merge and flow eastward around 36°N~38°N. At least in the surface waters, contaminated seawater affected by 1FNPP hardly flows southward across 38°N.[24] Distribution of ^{134}Cs inventories in seabed sediment (Fig. 4) showed a similar pattern to the simulation result of radiocesium-contained seawater at the early post-accident stage.[25-27] From these results, it can be considered that ^{134}Cs deposition to sediment associates with transport of contaminated seawater from 1FNPP.

In Figs. 5 (a) and (b), cumulative ^{134}Cs inventories in seabed sediment between 35°40’ N and 38°30’ N are plotted against the bottom depth and distance from 1FNPP, respectively. These figures indicate the following findings:

- In this region, cumulative inventories of ^{134}Cs in seabed sediment can be expressed as a function of bottom depth rather than that of distance from 1FNPP. The ^{134}Cs inventories decreased exponentially with increasing bottom depth.
- The decreasing rate of the ^{134}Cs inventory was lowered in the open ocean. A remarkable change was observed around 200 m depths.
- By extrapolating the relationship to the offshore, ^{134}Cs inventory approached to an insignificant level (i.e., detection limits) at 1400~1500 m depths.

The relationship between ^{134}Cs inventory and the bottom depth was defined as Eqs. (2) and (3).

$$I_z = 41356 \times e^{-0.0163z}, \qquad (z < 200\text{m}: r^2 = 0.72) \qquad (2)$$

$$I_z = 3412 \times e^{-0.00307z}, \qquad (z \geq 200\text{m}: r^2 = 0.57) \qquad (3)$$

where, I_z is the ^{134}Cs inventory in sediment per unit area (Bq/m^2) at bottom depth z (m). Since the relationship between ^{134}Cs inventory and bottom depth changes at 200 m depth (Fig. 5a), two equations were defined here. Data obtained from the "marginal" region (bottom depth: 200±20 m) were applied for both equations.

The distributional pattern of ^{134}Cs in seabed sediment indicates that accumulation processes of radiocesium to the seabed were different between coastal regions and open ocean. Due to the higher concentration in the coastal regions of dissolved radiocesium in seawater, higher probabilities are expected to adsorb radiocesium to the coastal sediment. As shown in Fig. 3, radiocesium penetrates into the deeper layers of coastal sediments, and it is considered that mobility of the accident-derived radiocesium in sediment is low.[6] In the offshore region, on the other hand, contaminated seawater hardly affects directly to the seabed. Consequently, more ^{134}Cs can be accumulated in the coastal sediments compared with offshore regions.

3.3 Total amount of sedimentary ^{134}Cs in seabed sediment off Fukushima

Considering the distributional patterns of ^{134}Cs in sediment, the total amount of ^{134}Cs accumulated in sediment in the study area, where remarkable deposition was observed (indicated by dashed line in Fig. 4), was estimated. Applying the relationship between ^{134}Cs inventory and bottom depth (Eqs. (2) and (3)) to Eq (4), ^{134}Cs inventories were integrated for eight depth ranges listed in Table 2.

$$I_{a\text{-}b} = \frac{1}{(b-a)}\int_a^b Iz\, dz. \qquad (4)$$

$I_{a\text{-}b}$ (Bq/m^2) is the mean ^{134}Cs inventory per unit area at a depth range between a (m) and b (m). Amount of ^{134}Cs in each depth range (Bq) was calculated by multiplying $I_{a\text{-}b}$ by the bottom area of the corresponding depth range. As topography data, the 1 minute Gridded Global Relief Data (ETOPO2v2) [28] were used here. The sum of ^{134}Cs amounts at the eight depth ranges was regarded as the total ^{134}Cs inventory in seabed sediment in the study area.

This estimation does not include data in the area within a 20 km radius from 1FNPP due to restriction of entrance for research vessels into the area in the early post-accidental stage. From observations in October 2011, TEPCO reported that concentration ^{134}Cs in seabed sediments within 20 km radius ranged between 9 and 918 Bq/kg-wet (194 Bq/kg-wet in average; n=10)[29]. Applying a conversion factor from wet- to dry-based concentration for this region (1.4), [30] the averaged ^{134}Cs in sediment is calculated to be 271 Bq/kg-dry. This concentration is about twice as those at coastal stations listed in Table 1 (119 Bq/kg in average, n=7). Sea area within the 20 km radius from 1FNPP (6.3×10^8 m^2) corresponds to 1.8% of the total area in Table 2 (3.5×10^{10} m^2). Accordingly, the seabed sediments within the 20 km radius may raise total ^{134}Cs amount by 4%. Although TEPCO also reported that more than 2000 Bq/kg-wet of ^{134}Cs was detected from seabed sediment adjacent to 1FNPP (< 1km from the facility),[31] the area is quite limited. High-resolution observations, carried out within 20 km radius from 1FNPP using an in-situ gamma detector, found that such a high concentrations of radiocesium is unevenly distributed with the size between several and tens of meters.[32,33] Because the expected increase of ^{134}Cs amount is much smaller than uncertainty of ^{134}Cs inventories estimated by Eqs. (2) and (3), we applied them for all areas including the area within the 20 km radius.

The total ^{134}Cs amount in sediment was estimated to be $2.0\pm0.6\times10^{14}$ Bq (Table 2). It is estimated that $[3.5\sim3.6]\times10^{15}$ Bq of ^{137}Cs was discharged directly from the 1FNPP facility to the ocean.[25,26] Kobayashi et al.[35] estimated that the cumulative deposition of ^{137}Cs from the atmosphere to the ocean surface between March and July 2011 was 7.4×10^{15} Bq. Since $^{134}Cs/^{137}Cs$ released by the accident is about 1.0 (as of March 11, 2011),[2] initial supply of ^{134}Cs to the North Pacific is calculated to be 11×10^{15} Bq. From these results, about 2% of the initial supply of ^{134}Cs to the ocean is accumulated in the seafloor.

Ito et al.[35] estimated that the amount of sedimentary ^{137}Cs in the Japan Sea (a marginal sea in the western North Pacific) consists of 3.8% of the total amount of ^{137}Cs (including dissolved and sedimentary ^{137}Cs) in the sea. Most of the ^{137}Cs was supplied by global fallout and the following lateral transport between 1950s and 2000s. Although the spatial and temporal scales are different from the 1FNPP's case, it is reasonable that several % of radiocesium is accumulated to the seafloor.

3.4 Accumulation processes of radiocesium to sediment in the coastal region

Results in Table 2 also indicate that more than 90% of sedimentary ^{134}Cs is accumulated on the coastal region (<200 m). The accumulation of ^{134}Cs was remarkable especially in the nearshore (<100 m) regions. In order to understand the dominant factors controlling the initial deposition of radiocesium to the seabed, it is important to outline the accumulation processes in the coastal regions. In the following subsections, potential amounts of ^{134}Cs supplied to the coastal sediment are estimated for three dominant processes as follows: (1) riverine input of radiocesium; (2) biological uptake and sinking to the seabed, (3) adsorption of dissolved radiocesium onto the surface of suspended particles/sediment. The integration period for the estimation is from March 23 (the day when the first significant concentration of accident-derived radionuclides was observed from seawater) to October 31, 2011.

3.4.1 Riverine input of radiocesium

Compared to a saltwater system, accumulation of radiocesium in particulate materials is more efficient in a freshwater system.[36] Unfortunately, little is known about radiocesium concentration in the suspended materials in river water at the post-accident stage of the 1FNPP accident. In addition, for most rivers flowing into this study area, stations used for observations of the flow rates as well as water levels had not been operating due to the damage from the tsunami that occurred on March 11, 2011.

Yamaguchi et al.[37] compiled monitoring data of radiocesium in soil, and estimated that 1.5 PBq of ^{134}Cs was accumulated on land within 80 km radius from 1FNPP until July, 2011. By time-series observations of at contaminated watersheds in Fukushima, it was estimated that ~0.5% of the accident-derived radiocesium in the watersheds was discharged during 2011.[38] From these parameters, the amount of ^{134}Cs supplied from rivers to the Pacific coast until the end of October 2011 is calculated to be 7.5×10^{12} Bq (Fig. 6). This amount is much smaller than amount of sedimentary ^{134}Cs in the coastal region (<200 m: $1.9\pm0.6\times10^{14}$ Bq, Table 2). In general, radiocesium supplied in a watershed is accumulated in the riverbed,[39] and the riverine transport of radiocesium to estuaries mainly occurs during flood events.[38,40] Typhoon “Roke” in September 2011 actually induced a large suspended flux to the study area, but no significant increase of radiocesium inventories in coastal sediment was observed.[6] This result indicates that such a sporadic supply of suspended ^{134}Cs within half a year after the accident was smaller than the above-mentioned estimation. However, continuous monitoring of the riverine input of radiocesium to the coastal regions is highly recommended considering that watersheds in the surrounding regions of 1FNPP accumulated high levels of radiocesium.

3.4.2 Biological uptake of radiocesium and sinking to the seabed

A significant levels of the accident-derived radiocesium was detected from lower trophic levels of marine biota such as zooplankton.[25,41] It is well known that such biogenic materials are considered as a carrier of the radionuclides.[9-11]

Concentration factors (*CF*), the relative concentration in biota to that of the ambient seawater, is widely used as a parameter in modeling interactions between the living organisms and seawater of an element/nuclides. By using a recommended *CF* values (100 L/Kg for Cs)[18] and ^{134}Cs concentration in seawater, ^{134}Cs concentration in biogenic particles under equilibrium conditions can be estimated. As shown in Fig. 7, ^{134}Cs concentrations in surface seawater decreased with time,[4] and an averaged concentration of the ^{134}Cs concentration between March and October 2011 within 100 km radius from 1FNPP was about 3 Bq/L. As the recommended *CF* value is based on wet weight of organisms or particles, considering the water content of the materials (c.a. 90%) [42,43], averaged ^{134}Cs concentration of biogenic particles is estimated to be 2,800 Bq/kg by dry weight.

An annual mean mass flux of sinking particles observed by a sediment trap experiment carried out from August 2011 to July 2012 at Sta. K8 is 0.5 g/m^2/d (observed at 100 m above the bottom: Otosaka, unpublished data). As a ^{210}Pb-based mass accumulation rate at coastal stations (Stas. J7, J9, K1 and K9) was about 1~15 times higher than the offshore station K8, the mass flux in the coastal regions is estimated to be ~7.5 g/m^2/d. Assuming that 80% of sinking particles consists of biogenic materials,[44] the downward flux of the biogenic particles is calculated to be ~6.0 g/m^2/day.

From these parameters and the area of the coastal region, 1.5×10^{10} m^2 (<200 m depth, Table 2), cumulative amount of ^{134}Cs supplied to the coastal seafloor by sinking biogenic particles until the end of October 2011 is calculated to be ~6×10^{13} Bq (Fig. 6). This amount is approximately equivalent to 35% of the amount of sedimentary ^{134}Cs in the coastal region. It can be concluded that sinking of biogenic particles is a minor mechanism to accumulate radiocesium to the coastal seafloor.

3.4.3 Adsorption of dissolved radiocesium to suspended particles and seabed sediment

Concentrations of radiocesium in seawater increased in the three months after the accident, and decreased by two orders of magnitude in the next three months (Fig. 7). In these periods, radiocesium concentrations in the seabed sediment also increased over three orders of magnitude, but decreased only one order.[5,6] These results indicate that, although surface waters actually have direct affected on the seabed, a seawater-sediment equivalent of radiocesium has not been established in half a year after the accident. Nevertheless, in a closed system, seawater-sediment equivalent of radiocesium can be established within several days,[45] and desorption of radiocesium from sediment is quite slow.[6] Contacting of the bottom waters with the seabed sediments over in half a year after the accident can lead to efficient adsorption of radiocesium to the sediment.

As described in subsection 3.1, sediment surface was disturbed by tsunami and a large amount of suspended particles existed in the coastal region over a few months after March 11, 2011. Repeated aftershocks would affect on the redistribution of the sediments. We therefore can consider that these processes also enhanced particle-seawater interactions and accumulation of radiocesium in the seabed sediment.

For the estimation the amount of adsorption of ^{134}Cs onto seabed, the following scenarios controlling initial deposition of radiocesium to the seabed can be assumed;

- An equilibrium between the bottom water and seabed sediment was established through the sediment-water interface,
- An equilibrium between the contaminated seawater and suspended particles was also established and the suspended particles settled to the seabed, and
- Both processes accumulated ^{134}Cs in sedimentary layer with 1 cm in thickness.

Based on these assumptions, potential amount of ^{134}Cs deposition is estimated using typical parameters such as, distribution coefficient (K_d) between sediment and seawater (3,500 L/kg)[18], and bulk density of sediment (0.5~1.5 kg/L: Appendix). Concentration of ^{134}Cs in the bottom water was calculated by the ^{134}Cs concentration in the surface water (Fig. 7) and C_z/C_0 values (Fig. 8). The C_z/C_0 is defined as a ratio of ^{134}Cs concentration in seawater at water depth z (m) to that in the surface water, and the values were about 1 in the coastal waters (<200m depth: Fig.8). We here adopted 0.1 as C_z/C_0 with a lower estimation, and obtained 0.3 Bq/L as an averaged ^{134}Cs concentration in the bottom water.

Estimated amount of ^{134}Cs accumulation per unit area of sediment ranges 5.2×10^3 and 1.6×10^4 Bq/m^2. As the area of the coastal region (<200 m depth) is 1.5×10^{10} m^2 (Table 2), the total amount of ^{134}Cs supplied by this process is estimated to be 8×10^{13}~ 2×10^{14} Bq (Fig. 6). It is reported that processes such as diffusion of bottom water across the seawater-sediment interface, bioturbation, and turbulence of the sediment surface can accumulate radionuclides in the middle layers (~10 cm) of sediment.[46-48] Therefore, the total amount estimated here might be underestimated. Nevertheless, this amount adequately supports the total inventory in the coastal region (Table 2: 1.9×10^{14} Bq), and this process is a more reasonable process to accumulate radiocesium to the seabed.

5. Summary

With respect to radiocesium released by the accident of 1FNPP, distributional patterns and their accumulation processes in the surrounding region of the plant are summarized as follows;

Sedimentation of the accident-derived radiocesium mainly occurred in the region off Fukushima, Miyagi and Ibaraki prefectures (35.7°N~38.5°N). As of November 2011, 0.2 PBq of ^{134}Cs, corresponding to about 2% of the accident-derived ^{134}Cs discharged to the marine environment, was accumulated in the seabed sediment.

More than 90% of the sedimentary radiocesium was accumulated in the coastal regions with water depth shallower than 200 m depth. It can be inferred that the primary process that derived the preferential accumulation of radiocesium to the coastal seafloor was adsorption of dissolved radiocesium to suspended particles or the sediment surface. This process is attributable to advection of contaminated seawater near the seabed of the regions during the post-accident stage within half a year after the accident.

Although downward transport of particulate radiocesium by biogenic particles seems to be a minor process in the coastal region, it might play a significant role in the offshore region. Remineralization and/or lateral transport of sedimentary radiocesium will become primary processes in redistributing of the radiocesium in the future.

As a process accumulating radiocesium to the seabed in the coastal regions, supply of radiocesium through rivers would not be significant at least in the post accidental stage. Nevertheless, continuous monitoring of the land-sea fluxes of radiocesium is highly recommended.

Acknowledgements

Field supports were provided by captains, crews and researchers of R/V Hakuho-maru KH11-07, R/V Tansei-maru KT-11-27 cruises. This investigation benefited enormously and was vastly improved through discussions with Drs. T. Gamo, M. Uematsu, H. Obata, J. Nishikawa (Univ of Tokyo), S. Igarashi (Fukushima pref.), M. Ikeda (Hokkaido Univ.), J. Kanda (Tokyo Univ. Mar. Sci. Technol.), H. Narita (Tokai Univ.), J. Zhang, K. Horikawa (Univ. of Toyama), S. Nagao (Kanazawa Univ.), M. Aoyama (MRI., Japan) T. Kobayashi, H. Kawamura and T. Suzuki (JAEA). We are also grateful to the two anonymous reviewers for their constructive and helpful comments. This work was partially supported by Grant-in-Aid for Scientific Research on Innovative Areas (#24110004) to YK.

References

1. MEXT (Ministry of Education, Culture, Sports, Science and Technology, Japan). 2011a. http://radioactivity.nsr.go.jp/ja/contents/4000/3857/24/1305744_0527.pdf
2. K.O. Buesseler, Impacts of the Fukushima Nuclear Power Plants on marine radioactivity. *Environmental Science and Technology,* 2011, **45**, 9931-9935.
3. M. Aoyama, D. Tsumune, M. Uematsu, F. Kondo, Y. Hamajima. Temporal variation of ^{134}Cs and ^{137}Cs activities in surface water at stations along the coastline near the Fukushima Dai-ichi Nuclear Power Plant accident site, Japan. *Geochem. J*., 2012, **46**, 321-325.
4. S. Oikawa, H. Takata, T. Watabe, J. Misonoo, M. Kusakabe. Distribution of the Fukushima-derived radionuclides in seawater in the Pacific off the coast of Miyagi, Fukushima, and Ibaraki Prefectures, Japan, *Biogeosci.*, 2013, **10**, 5031-5047.
5. M. Kusakabe, S. Oikawa, H. Takata, J. Misonoo. Spatiotemporal distributions of Fukushima-derived radionuclides in surface sediments in the waters off Miyagi, Fukushima, and Ibaraki Prefectures, Japan. *Biogeosci*., 2013, **10**, 4819-4850.
6. S. Otosaka, T. Kobayashi. Sedimentation and remobilization of radiocesium in the coastal area of Ibaraki, 70 km south of the Fukushima Dai-ichi Nuclear Power Plant, *Environ. Monit. Assess.*, 2013, **185**, 5419-5433.
7. R.N.J. Comans, M. Haller, P. DePreter. Sorption of cesium on illite: Non-equilibrium behavior and reversibility. *Geochim. Cosmochim. Acta*, 1991, **55**, 433-440.
8. C. Poinssot, B. Baeyens, M.H. Bradbury: Experimental and modeling studies of caesium sorption on illite, *Geochim. Cosmochim. Acta*, 1999, **63**, 3217-3227.
9. S.W. Fowler, P. Buat-Menard, Y. Yokoyama, S. Ballestra, E. Holm, H.V. Nguyen. Rapid removal of Chernobyl fallout from Mediterranean surface waters by biological activity. *Nature,* 1987, **329**, 56-58.
10. M. Kusakabe, T.L. Ku, K. Harada, K.Taguchi, S. Tsunogai. Chernobyl radioactivity found in mid-water sediment trap interceptor in the N. Pacific and Bering Sea. *Geophys. Res. Lett*., 1988, **15**, 44-47.
11. M. C. Honda, H. Kawakami, S. Watanabe, T. Saino. Concentration and vertical flux of Fukushima-derived radiocesium in sinking particles from two sites in the Northwestern Pacific Ocean. *Biogeosci.*, 2013, **10**, 3525–3534.
12. K.O. Buesseler, Fishing for answers off Fukushima, *Science*, 2012, **338**, 480.
13. Y. Tateda, D. Tsumune, T. Tsubono. Simulation of radioactive cesium transfer in the southern Fukushima coastal biota using a dynamic food chain transfer model. *J. Environ. Radioactiv*., 2013, **124**, 1-12.
14. T. Wada, Y. Nemoto, S. Shimamura, T. Fujita, T. Mizuno, T. Sohtome, K. Kamiyama, T. Morita, S.

Igarashi. Effects of the nuclear disaster on marine products in Fukushima. *J. Environ. Radioactiv.,* 2013, **124**, 246-254.

15. Z. Baumann, N. Casacuberta, H. Baumann, P. Masqué, N.S. Fisher. Natural and Fukushima-derived radioactivity in macroalgae and mussels along the Japanese shoreline. *Biogeosci*., 2013, **10**, 3809–3815.
16. IAEA (International Atomic Energy Agency). *Collection and preparation of bottom sediment samples for analysis of radionuclides and trace elements*. IAEA-TECDOC, 1360, Vienna, 1993.
17. K. Aoyagi, C. Igarashi. On the size distribution of sediments in the coastal sea of Fukushima Prefecture. *Bull. Fukushima Pref. Fish. Exp. Sta*., 1999, **8**, 69-81 (in Japanese).
18. D.A. Stanners, S.R. Aston. Desorption of ^{106}Ru, ^{134}Cs, ^{137}Cs, ^{144}Ce and ^{241}Am from intertidal sediment contaminated by nuclear fuel reprocessing effluents. *Estuarine Coastal and Shelf Sci*., 1982, **14**, 687-691.
19. N.G. Alexandeopoulos, T. Alexandropoulou, D. Anagnostopoulos, E.Evangelou, J.T. Kotsis, I. Theodoridou. Chernobyl fallout on Ioannina, Greece. *Nature*, 1986, **322**, 779.
20. UNSCEAR, *Sources and effects of ionizing radiation*. UNSCEAR 2000 Report, Scientific Annex C, United Nations, New York, 2000
21. E. Seibold and W.H. Berger, in *The Sea Floor: An Introduction to Marine Geology*, Springer-Verlag, New York, 3rd edn., 1996, ch. 4, pp. 97-125.
22. K. Hanawa, H. Mitsudera. Variation of water system distribution in the Sanriku coastal area. *J. Oceanogr. Soc. Japan*, 1987, **42**, 435-446.
23. H. Kubo. Research on the oceanographic conditions of Kashima-Nada, off the east coast of Honshu. *Bull. Ibaraki Pref. Fish. Exp. Sta*., 1988, **26**, 1-98 (in Japanese with English summary and captions).
24. K.O. Buesseler, S.R. Jayne, N.S. Fisher, I.I. Rypina, H. Baumann, Z. Baumann, C.F. Breier, E.M. Douglass, J. George, A.M. Macdonald, H. Miyamoto, J. Nishikawa, S.M. Pike, S. Yoshida. Fukushima-derived radionuclides in the ocean and biota off Japan. *Proc. Natl. Acad. Sci.*, 2012, **109**, 5984-5988.
25. H. Kawamura, T. Kobayashi, A. Furuno, T. In, Y. Ishikawa, T. Nakayama, S. Shima, T. Awaji. Preliminary numerical experiments on oceanic dispersion of ^{131}I and ^{137}Cs discharged into the ocean because of the Fukushima Daiichi Nuclear Power Plant Disaster. *J. Nucl. Sci. Technol.*, 2011, **48**, 1349-1356.
26. D. Tsumune, T. Tsubono, M. Aoyama, K. Hirose. Distribution of oceanic ^{137}Cs from the Fukushima Dai-ichi Nuclear Power Plant simulated numerically by a regional ocean model. *J. Environ. Radioact.*, 2012, **111**, 100-108.
27. Y. Masumoto, Y. Miyazawa, D. Tsumune, T. Tsubono, T. Kobayashi, H. Kawamura, C. Estournel, P.

Marsaleix, L. Lanerolle, A. Mehra, Z.D. Garraffo. Oceanic dispersion simulations of ^{137}Cs released from the Fukushima Daiichi Nuclear Power Plant. *Elements*, 2012, **8**, 207-212.

28. NOAA (National Oceanic and Atmospheric Administration). *1-minute Gridded Global Relief Data (ETOPO2v2)*. NOAA National Geophysical Data Center, Boulder, 2006.
29. TEPCO: 2011b. http://radioactivity.nsr.go.jp/ja/list/280/list-201110.html
30. TEPCO: 2011c. http://radioactivity.nsr.go.jp/ja/contents/6000/5591/24/229_0625.pdf
31. TEPCO (Tokyo Electric Power Co.): 2011a. http://radioactivity.nsr.go.jp/ja/contents/5000/4623/24/1307070_071610d.pdf
32. B. Thornton, S. Ohnishi, T. Ura, N. Odano, S. Sasaki, T. Fujita, T. Watanabe, K. Nakata, T. Ono, D. Ambe. Distribution of local 137Cs anomalies on the seafloor near the Fukushima Dai-ichi Nuclear Power Plant. *Mar. Pollution Bull.*, 2013, **74**, 344–350.
33. B. Thornton, S. Ohnishi, T. Ura, N. Odano, T. Fujita. Continuous measurement of radionuclide distribution off Fukushima using a towed sea-bed gamma ray spectrometer. *Deep-sea Res. I*, 2013, **79**, 10–19.
34. T. Kobayashi, H. Nagai, M. Chino, H. Kawamura: Source term estimation of atmospheric release due to the Fukushima Dai-ichi Nuclear Power Plant accident by atmospheric and oceanic dispersion simulations. *J. Nucl. Sci. Technol.*, 2013, **50**, 255-264.
35. T. Ito, S. Otosaka, H. Kawamura. Estimation of total amounts of anthropogenic radionuclides in the Japan Sea. *J. Nucl. Sci. Technol.*, 2007, **44**, 912-922.
36. IAEA. *Sediment distribution coefficients and concentration factors for biota in the marine environment*. IAEA Technical Report Series 422, Vienna, 2004.
37. M. Yamaguchi, K. Maekawa, S. Takeuchi, A. Kitamura, Y. Onishi. Development of a model to predict a radionuclide distribution based on soil migration after Fukushima Dai-ichi Nuclear Power Plant accident. *J. Nucl. Fuel Cycle Environ.*, 2014, in press (in Japanese with English abstract).
38. S. Ueda, H. Hasegawa, H. Kakiuchi, N. Akata, Y. Ohtsuka. Fluvial discharges of radiocaesium from watersheds contaminated by the Fukushima Dai-ichi Nuclear Power Plant accident, Japan. *J. Enriron. Radioactiv.*, 2013, **118**, 96-104.
39. T. Matsunaga, H. Amano, N. Yanase. Discharge of dissolved and particulate ^{137}Cs in the Kuji River, Japan. *Appl. Geochem.*, 1991, **6**, 159-167.
40. S. Nagao, M. Kanamori, S. Ochiai, S. Tomihara, K. Fukushi, M. Yamamoto. Export of ^{134}Cs and ^{137}Cs in the Fukushima river systems at heavy rains by Typhoon Roke in September 2011. *Biogeosci.*, 2013, **10**, 6215-6223.
41. M. Kitamura, Y. Kumamoto, H. Kawakami, E. C. Cruz, K. Fujikura. Horizontal distribution of Fukushima-derived radiocesium in zooplankton in the northwestern Pacific Ocean. *Biogeosci.*, 2013,

10, 5729-5738.

42 H.H. Hannan, T.C. Dorris. Succession of a macrophyte community in a constant temperature river. *Limnol. Oceanogr.*, 1970. **15**, 442-453.

43 V. Sladecek, A. Sladeckova. Relationship between wet weight and dry weight of the periphyton. *Limnol. Oceanogr.*, 1963, **8**, 309-311.

44 S. Otosaka and S. Noriki. Relationship between Composition of Settling Particles and Organic Carbon Flux in the Western North Pacific and the Japan Sea. *J. Oceanogr.*, 2005, **61**, 25-40.

45. U.P. Nyffeler, Y.-H. Li, P.H. Santschi. A kinetic approach to describe trace-element distribution between particles and solution in natural aquatic systems. *Geochim. Cosmochim. Acta*, 1984, **48**, 1513-1522.

46 P.H. Santschi, P.Bower, U.P. Nyffeler, A. Axevedo, W.S. Broecker. Estimates of the resistance to chemical transport posed by the deep-sea boundary layer. *Limnol. Oceanogr*. 1983, **28**, 899-912.

47 K.M. Yeager, P.H. Santschi, G.T. Rowe. Sediment accumulation and radionuclide inventories (^{239,240}Pu, ^{210}Pb and ^{234}Th) in the northern Gulf of Mexico, as influenced by organic matter and macrofaunal density. *Marine Chemistry*, 2004, **91**, 1–14.

48 F. Dufois, R. Verney, P. LeHir, F. Dumas, S. Charmasson. Impact of winter storms on sediment erosion in the Rhone River prodelta and fate of sediment in the Gulf of Lions (North Western Mediterranean Sea). *Continental Shelf Res.*, 2014, **72**, 57-72.

Figure captions

Fig. 1 Sampling stations

Fig. 2 Vertical changes in bulk density, $^{210}Pb_{xs}$, organic matter content and ^{134}Cs concentration at (a) Sta. J7, (b) Sta.J8, and (c) Sta.FS1. Fig.(d) shows lateral distribution of the three sedimentary patterns. In Fig. (d), open triangles, closed triangles, and crosses indicate stations at where sedimentary pattern I, II and III was observed, respectively. See text for the sedimentary patterns.

Fig. 3 $F_{0\text{-}3}$ values as a function of bottom depth.

Fig. 4 Distribution of sedimentary ^{134}Cs. In this paper, the "total" amount of sedimentary ^{134}Cs was estimated for the area inside the dashed line.

Fig. 5 ^{134}Cs inventories as a function of (a) bottom depth and (b) distance from 1FNPP. Data are obtained in October and November 2011, except for two offshore data obtained in August 2011. Activities are decay corrected to March 11, 2011. Solid lines in Fig. (a) indicate regression lines between the two parameters for continental shelf (<200 m) and the outer (>200 m) regions. Dashed line indicates lowest level of significant ^{134}Cs inventory estimated from detection limit of gamma counting.

Fig. 6 Expected accumulation processes of radiocesium in the coastal region. Total amount denotes cumulative ^{134}Cs amount from 0m to 200m (Table 2). See text for estimated ^{134}Cs supply with each process.

Fig. 7 Temporal change in ^{134}Cs concentration in surface seawater within 100 km radius from 1FNPP. Data are from Oikawa et al.[4], and decay-corrected to March 11, 2011. Horizontal lines indicate representative values used in the calculation in subsection 3.3.2.

Fig. 8 Vertical distribution of the C_z/C_0 value. Data are from Oikawa et al. (2013)[4] obtained within 100 km radius from 1FNPP, and decay-corrected to March 11, 2011. The C_z/C_0 value is defined as a ratio of ^{134}Cs concentration in seawater at water depth z to that in the surface. Horizontal line indicates the representative value used in the calculation in subsection 3.3.3 ($C_z/C_0 = 0.1$).

Table captions

Table 1 Locations of sampling station, ^{134}Cs and ^{137}Cs inventories, $F_{0\text{-}3}$ values, and sediment properties.

Table 2 Table 2 Amount of sedimentary ^{134}Cs in the North Pacific between 35°40' N and 38°30' N

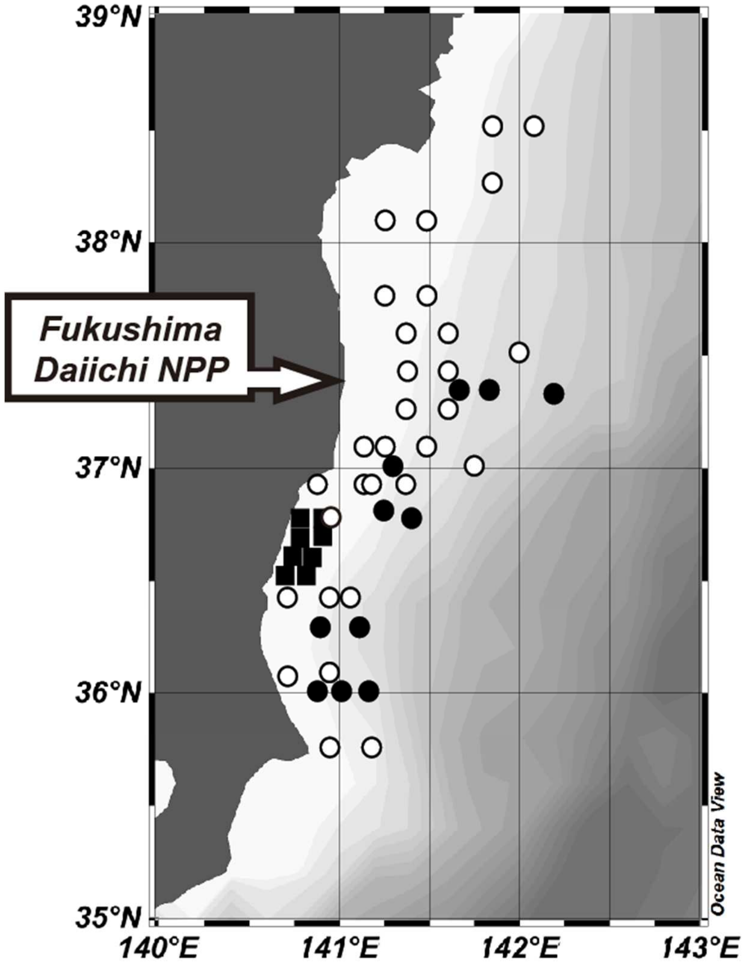

Otosaka and Kato, Fig. 1

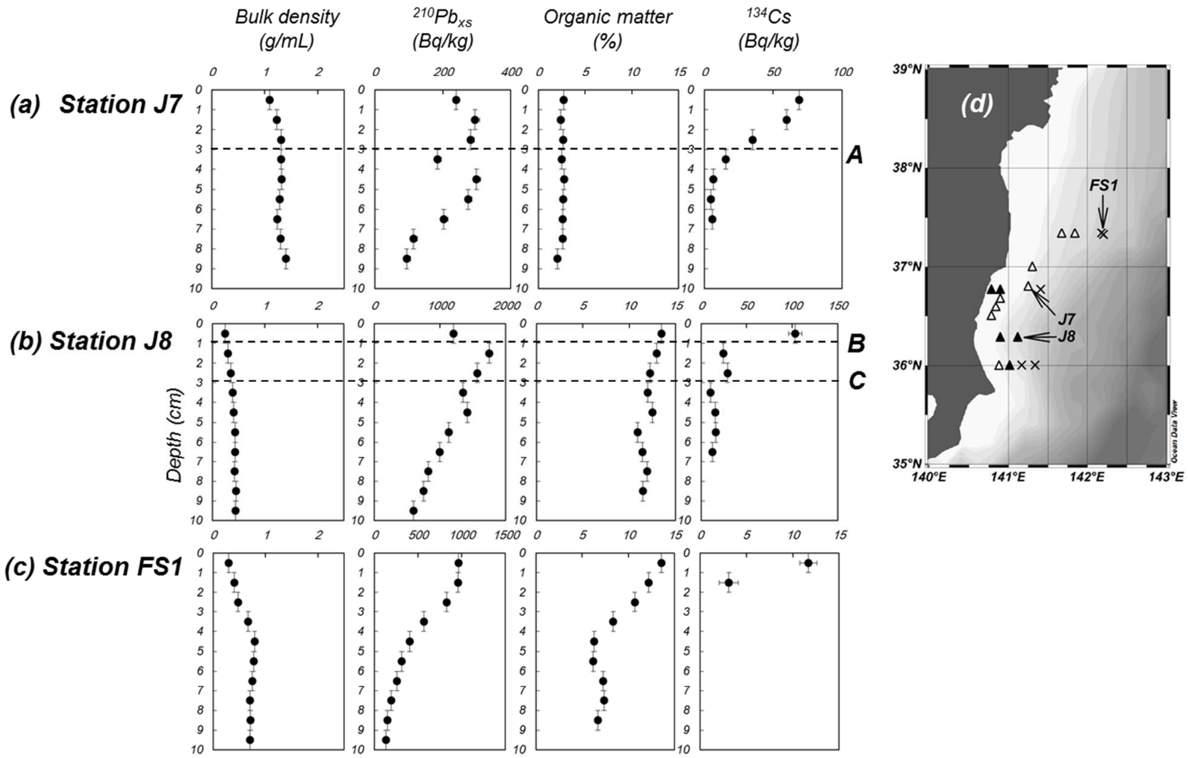

Otosaka and Kato, Fig. 2

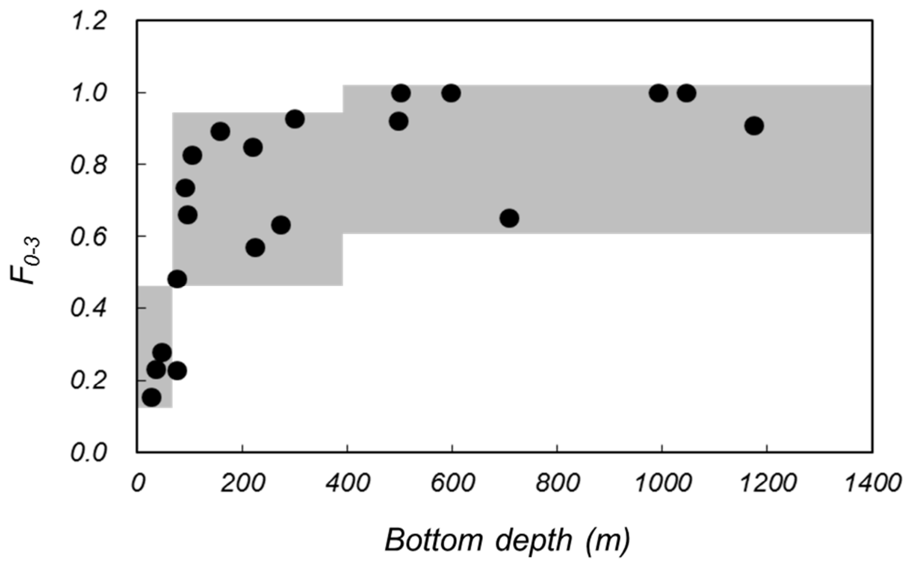

Otosaka and Kato, Fig. 3

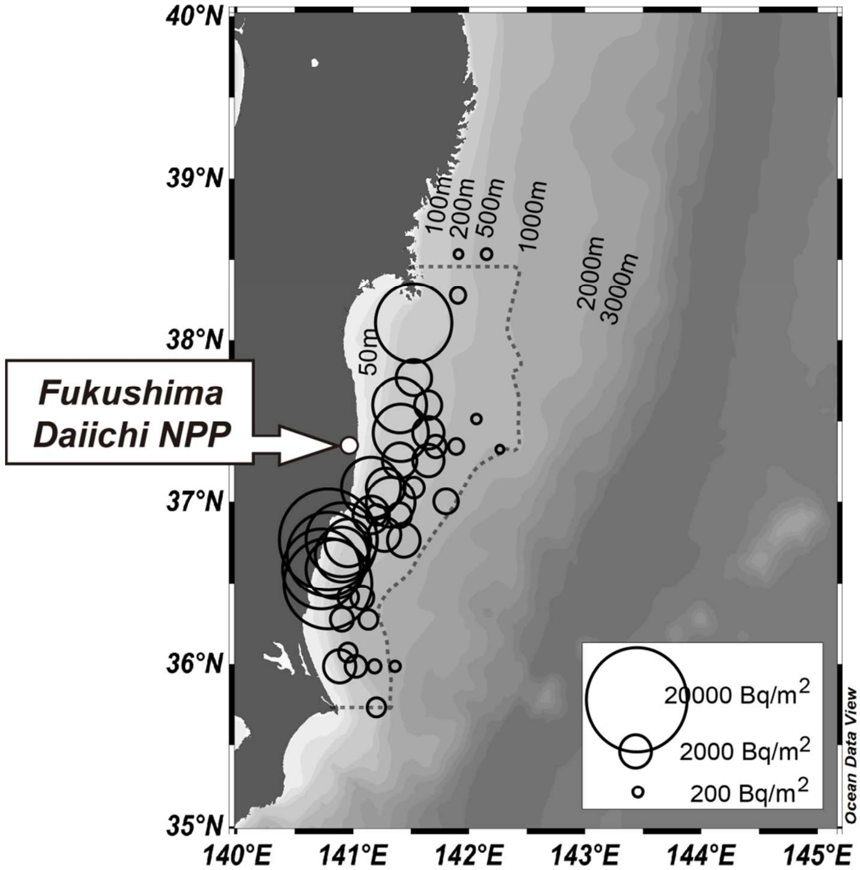

Otosaka and Kato, Fig. 4

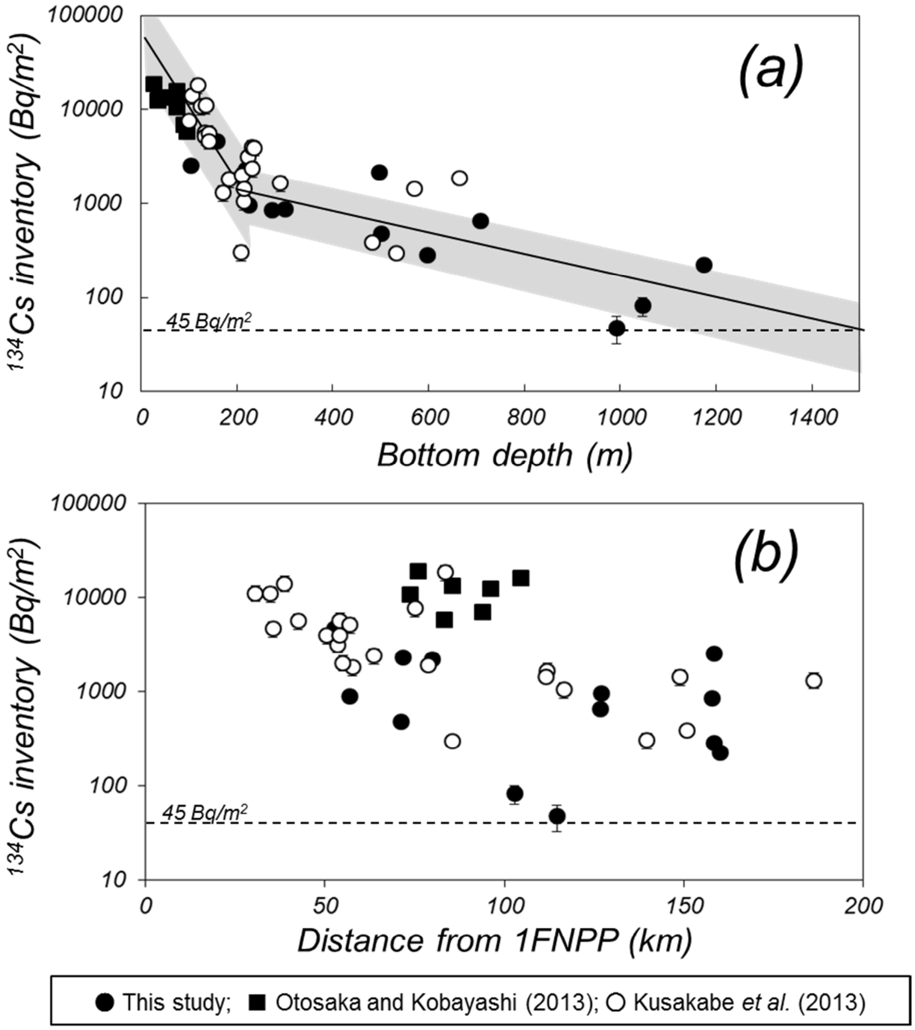

Otosaka and Kato, Fig. 5

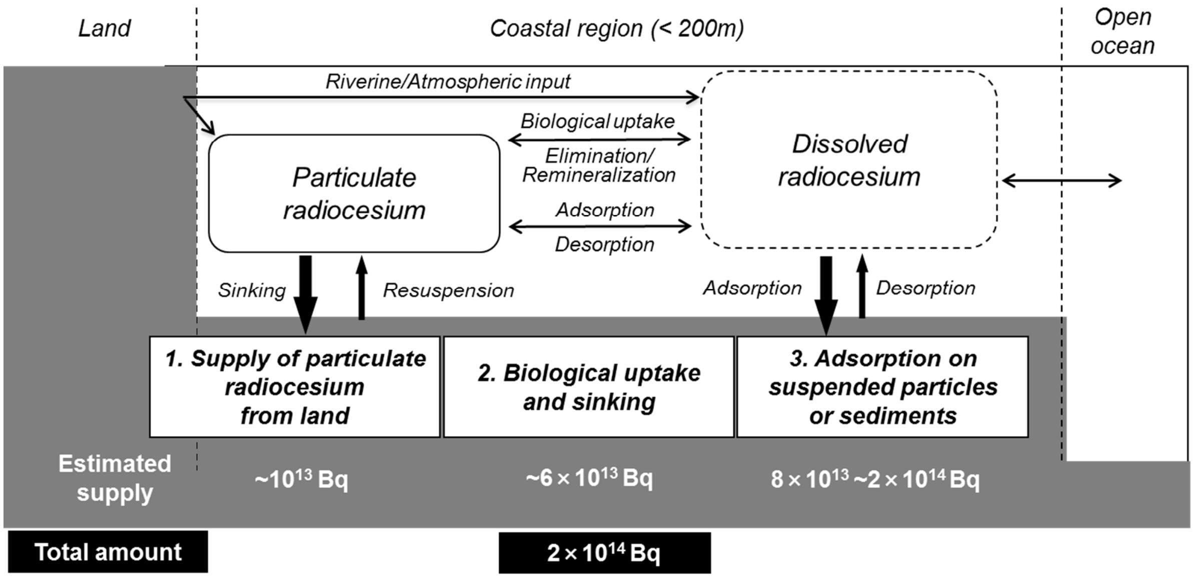

Otosaka and Kato, Fig. 6

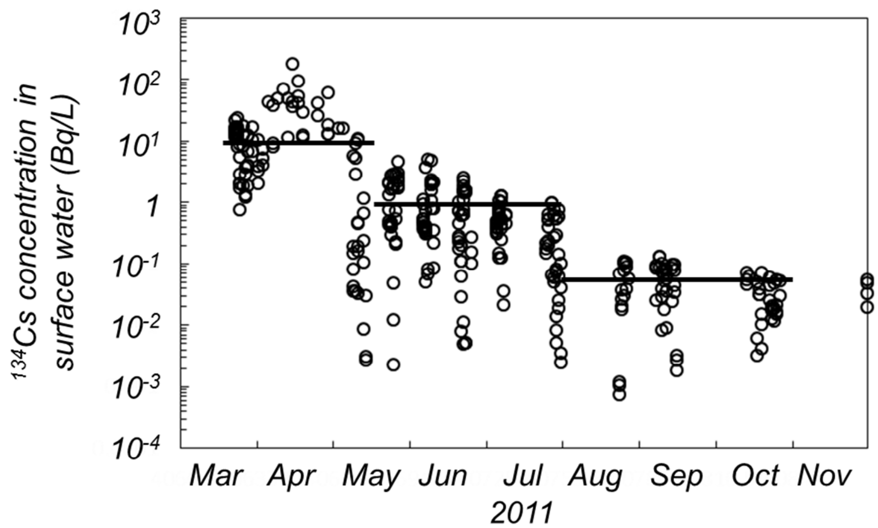

Otosaka and Kato, Fig. 7

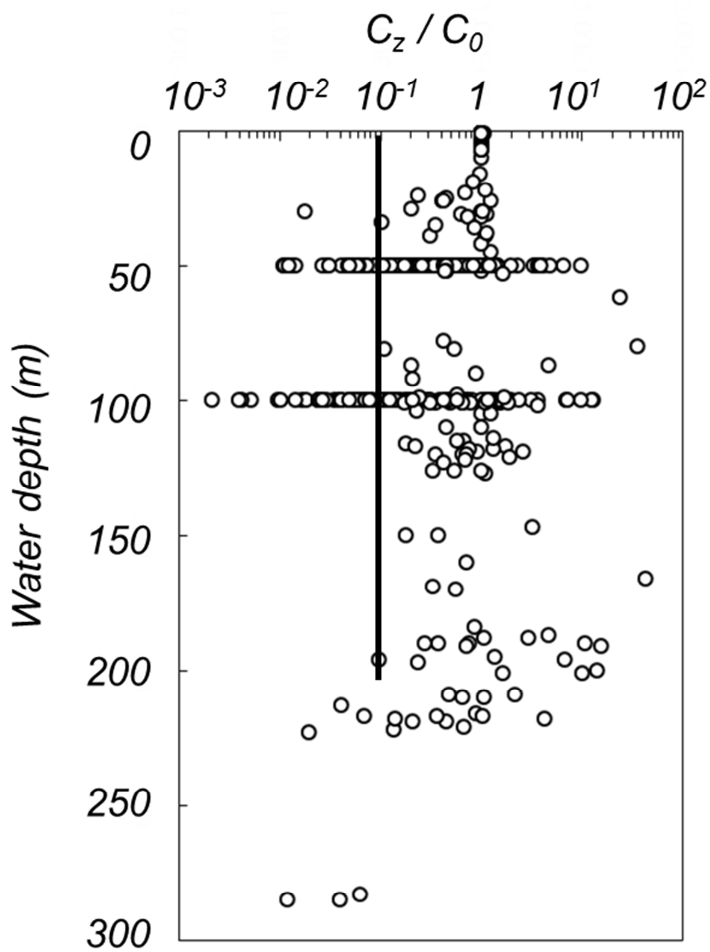

Otosaka and Kato, Fig. 8

Table 1 Locations of sampling station, ^{134}Cs and ^{137}Cs inventories, $F_{0\text{-}3}$ values, and sediment properties.

Station	Sampling date	North latitude		East longitude		Depth	Data category[a]	Sediment pattern [b]	^{134}Cs inventory [c]	^{137}Cs inventory [c]	$F_{0\text{-}3}$ [b]	Org. matter	Wentworth size class [d]
		Deg	Min	Deg	Min	m			kBq/m^2	kBq/m^2		%	
K1	2011/11/1	36	0	140	53	105	A	I	2.52 ± 0.04	2.57 ± 0.03	0.83	4.8	Fine sand
K9	2011/10/31	36	60	141	18	158	A	I	4.61 ± 0.04	4.67 ± 0.04	0.89	3.7	Coarse silt
J7	2011/10/31	36	48	141	15	220	A	I	2.30 ± 0.04	2.23 ± 0.03	0.85	2.7	Medium sand
J9	2011/10/31	36	17	140	54	225	A	II	0.94 ± 0.03	1.04 ± 0.02	0.57	3.8	Fine sand
K2	2011/11/1	36	0	141	1	273	A	II	0.84 ± 0.05	0.90 ± 0.02	0.63	4.9	Very fine sand
K6	2011/10/29	37	20	141	40	300	A	I	0.87 ± 0.03	0.90 ± 0.02	0.93	3.7	Fine sand
J6	2011/10/31	36	46	141	24	497	A	III	2.16 ± 0.03	2.09 ± 0.03	0.92	9.7	Coarse silt
K7	2011/10/29	37	20	141	50	501	A	I	0.48 ± 0.02	0.46 ± 0.02	1.00	7.4	Very fine sand
K3	2011/11/1	35	60	141	10	597	A	III	0.28 ± 0.02	0.31 ± 0.02	1.00	9.3	Coarse silt
J8	2011/10/31	36	17	141	7	708	A	II	0.65 ± 0.03	0.71 ± 0.02	0.65	13.5	Coarse silt
FS1	2011/8/3	37	20	142	10	992	A	III	0.05 ± 0.01	0.10 ± 0.01	1.00	11.2	Coarse silt
K8	2011/10/29	37	19	142	12	1047	A	III	0.08 ± 0.01	0.10 ± 0.01	1.00	13.6	Coarse silt
FS5	2011/8/5	36	0	141	20	1175	A	III	0.22 ± 0.01	0.21 ± 0.01	0.91	13.0	Coarse silt
S4	2011/10/27	36	46	140	47	26	B	N/A	18.9 ± 0.8	19.1 ± 0.8	0.15	3.3	Very fine sand / Fine sand
S2	2011/10/27	36	35	140	44	35	B	N/A	12.4 ± 0.5	12.1 ± 0.5	0.23	5.6	Coarse silt - Granule
S3	2011/10/27	36	41	140	47	47	B	N/A	13.3 ± 0.5	13.3 ± 0.5	0.28	3.6	Fine sand / Medium sand
S5	2011/10/27	36	46	140	54	75	B	II	10.7 ± 0.4	10.1 ± 0.4	0.48	6.4	Very fine sand
S8	2011/10/27	36	30	140	47	75	B	I	16.0 ± 0.7	15.4 ± 0.6	0.23	3.4	Very fine sand / Fine sand
S7	2011/10/27	36	35	140	51	90	B	I	6.93 ± 0.28	6.56 ± 0.2	0.73	6.5	Very fine sand
S6	2011/10/27	36	41	140	54	95	B	II	5.78 ± 0.22	5.56 ± 0.2	0.66	6.6	Very fine sand
MEXT-I1	2012/10/25	36	45	140	57	99	C	N/A	7.6 ± 1. 9	8.0 ± 1.4	N/A	No data	No data
MEXT-G0	2012/10/22	37	5	141	8	107	C	N/A	13.7 ± 3.4	13.0 ± 2.3	N/A	No data	No data
MEXT-B3	2012/10/18	38	5	141	29	118	C	N/A	21.6 ± 5.4	21.3 ± 3.8	N/A	No data	No data
MEXT-D1	2012/10/18	37	35	141	22	124	C	N/A	10.1 ± 2.5	10. 6 ± 1.9	N/A	No data	No data
MEXT-C3	2012/10/18	37	45	141	29	133	C	N/A	4.5 ± 1.1	4.6 ± 0.8	N/A	No data	No data
MEXT-H1	2012/10/23	36	55	141	8	134	C	N/A	4.7 ± 1.2	4.7 ± 0.8	N/A	No data	No data
MEXT-E1	2012/10/19	37	25	141	23	135	C	N/A	11.0 ± 2.6	11.0 ± 2.0	N/A	No data	No data
MEXT-G1	2012/10/23	37	5	141	15	141	C	N/A	5.5 ± 1.4	5.4 ± 1.0	N/A	No data	No data
MEXT-F1	2012/10/19	37	15	141	22	142	C	N/A	4.0 ± 1.0	4.2 ± 0.8	N/A	No data	No data
MEXT-L3	2012/10/13	35	45	141	11	171	C	N/A	1.2 ± 0.3	1.2 ± 0.2	N/A	No data	No data
MEXT-I3	2012/10/25	36	55	141	11	184	C	N/A	1.3 ± 0.3	1.4 ± 0.2	N/A	No data	No data
MEXT-A1	2012/10/17	38	30	141	51	209	C	N/A	0.23 ± 0.06	0.24 ± 0.04	N/A	No data	No data
MEXT-G3	2012/10/23	37	5	141	29	210	C	N/A	1.4 ± 0.3	1.4 ± 0.3	N/A	No data	No data
MEXT-a1	2012/10/17	38	15	141	51	214	C	N/A	0.80 ± 0.20	0.81 ± 0.15	N/A	No data	No data
MEXT-K2	2012/10/13	36	5	140	57	215	C	N/A	1.2 ± 0.3	1.2 ± 0.2	N/A	No data	No data
MEXT-D3	2012/10/19	37	35	141	36	224	C	N/A	2.4 ± 0.6	2.5 ± 0.5	N/A	No data	No data

MEXT-E3	2012/10/22	37	25	141	36	232	C	N/A	3.0	±	0.8	3.2	±	0.6	N/A	No data	No data
MEXT-H3	2012/10/24	36	55	141	22	232	C	N/A	1.8	±	0.5	1.9	±	0.3	N/A	No data	No data
MEXT-F3	2012/10/23	37	15	141	36	236	C	N/A	3.1	±	0.8	3.2	±	0.6	N/A	No data	No data
MEXT-J2	2012/10/26	36	25	140	57	291	C	N/A	1.3	±	0.3	1.3	±	0.3	N/A	No data	No data
MEXT-A3	2012/10/17	38	30	142	5	483	C	N/A	0.25	±	0.07	0.26	±	0.06	N/A	No data	No data
MEXT-E5	2012/10/22	37	30	142	0	533	C	N/A	0.18	±	0.05	0.20	±	0.04	N/A	No data	No data
MEXT-J3	2012/10/25	36	25	141	4	570	C	N/A	1.1	±	0.3	1.2	±	0.2	N/A	No data	No data
MEXT-G4	2012/10/24	37	0	141	45	664	C	N/A	1.1	±	0.3	1.1	±	0.3	N/A	No data	No data

[a] See Method section for detail.
[b] See subsection 3.1 for detail.
[c] Decay corrected to March 11, 2011.
[d] Data of size class are on the surface sediment.
N/A: Data not available.

Table 2 Amount of sedimentary ^{134}Cs in the North Pacific between 35°40' N and 38°30' N

Depth range	Area		^{134}Cs amount*	
m	km^2	%	Bq	%
0-100	7.9×10^3	22	$[1.6 \pm 0.5] \times10^{14}$	81
100-200	6.6×10^3	19	$[2.6 \pm 0.8] \times10^{13}$	13
200-400	4.5×10^3	13	$[4.3 \pm 1.8] \times10^{12}$	2.9
400-600	3.5×10^3	9.9	$[2.6 \pm 1.1] \times10^{12}$	1.7
600-800	3.0×10^3	8.6	$[1.2 \pm 0.5] \times10^{12}$	0.8
800-1000	3.1×10^3	8.8	$[6.9 \pm 2.8] \times10^{11}$	0.4
1000-1200	2.9×10^3	8.1	$[3.4 \pm 1.4] \times10^{11}$	0.2
1200-1500	3.8×10^3	11	$[2.2 \pm 0.9] \times10^{11}$	0.1
Total	3.5×10^4	100	$[2.0 \pm 0.6] \times10^{14}$	100

*Decay corrected to March 11, 2011. Uncertainty is based on 95% confidence interval with relationship between ^{134}Cs inventories in sediment and water depth (Fig. 3).

Appendix. Concentrations of ^{134}Cs, ^{137}Cs and ^{210}Pb$_{xs}$ and bulk density of sediment.

Station	Sampling date	Layer	^{134}Cs concentration*			^{137}Cs concentration*			^{210}Pb$_{xs}$ concentration			Bulk density
		cm	Bq/kg			Bq/kg			Bq/kg			g/cm^3
K1	2011/11/1	0-1	159	±	2	193	±	2	413	±	12	0.71
		1-2	45.0	±	1.3	56.0	±	1.3	335	±	30	1.08
		2-3	5.9	±	0.7	7.7	±	0.7	243	±	28	1.20
		3-4	17.3	±	0.9	23.1	±	0.9	286	±	22	1.16
		4-5	3.8	±	0.7	5.8	±	0.6	269	±	19	1.22
		5-6	4.1	±	0.6	5.5	±	0.6	278	±	22	1.26
		6-7	2.4	±	0.6	3.7	±	0.6	238	±	22	1.30
		7-8	<0.9			1.6	±	0.5	227	±	19	1.30
		8-9	1.7	±	0.5	2.5	±	0.5	227	±	27	1.33
		9-10	<0.9			<0.7			210	±	22	1.32
K9	2011/10/31	0-1	116	±	1	144	±	1	224	±	9	1.07
		1-2	92.6	±	1.4	114	±	1	371	±	48	1.27
		2-3	68.0	±	1.3	82.3	±	1.4	146	±	45	1.33
		3-4	25.1	±	0.9	29.0	±	1.0	343	±	44	1.32
		4-5	5.8	±	0.9	8.1	±	1.0	326	±	44	1.32
		5-6	<0.9			6.8	±	0.8	286	±	44	1.29
		6-7	<0.9			<0.9			123	±	44	1.25
J7	2011/10/29	0-1	55.6	±	1.1	61.9	±	0.9	239	±	9	1.09
		1-2	48.3	±	1.0	49.0	±	0.9	295	±	14	1.23
		2-3	28.4	±	0.9	28.0	±	0.7	281	±	12	1.31
		3-4	12.6	±	0.9	16.8	±	0.7	184	±	12	1.31
		4-5	5.3	±	0.9	6.0	±	0.7	299	±	12	1.32
		5-6	3.9	±	0.9	8.2	±	0.7	275	±	12	1.28
		6-7	4.6	±	0.9	6.7	±	0.7	203	±	13	1.24
		7-8	<0.9			4.8	±	0.6	114	±	11	1.30
		8-9	<0.8			2.6	±	0.7	94	±	11	1.40
J9	2011/10/31	0-1	24.4	±	1.1	29.8	±	1.2	291	±	9	0.86
		1-2	17.8	±	1.0	23.8	±	1.0	394	±	34	0.98
		2-3	4.8	±	0.7	8.3	±	0.1	429	±	27	1.05
		3-4	2.5	±	0.7	4.8	±	0.7	429	±	26	1.08
		4-5	6.1	±	0.8	8.4	±	0.8	410	±	35	1.07
		5-6	12.1	±	0.9	15.4	±	0.8	457	±	26	1.05
		6-7	10.3	±	0.8	13.1	±	0.8	437	±	26	1.05
		7-8	<1.1			<0.9			352	±	22	1.10
K2	2011/11/1	0-1	20.2	±	1.6	28.9	±	1.3	382	±	11	0.79
		1-2	12.4	±	1.5	17.4	±	1.3	472	±	18	0.87
		2-3	17.8	±	1.3	24.6	±	1.2	407	±	15	0.90
		3-4	5.6	±	1.4	9.3	±	1.1	406	±	15	0.94
		4-5	<1.2			3.6	±	1.2	350	±	16	0.98
		5-6	4.7	±	1.3	5.3	±	1.1	363	±	15	1.00
		6-7	8.9	±	2.0	4.0	±	1.0	314	±	15	1.02
		7-8	<1.1			<0.9			184	±	15	1.05
		8-9	5.3	±	1.3	2.7	±	1.1	175	±	14	1.50
		9-10	<1.0			4.3	±	1.1	127	±	14	1.18
K6	2011/10/29	0-1	17.5	±	0.9	22.2	±	1.0	264	±	11	0.93
		1-2	31.4	±	1.3	39.3	±	1.0	182	±	7	1.00
		2-3	16.7	±	0.9	20.4	±	0.9	206	±	8	1.07
		3-4	4.2	±	0.7	5.3	±	0.7	167	±	7	1.13

		4-5	<1.1			2.4	±	0.7	156	±	7	1.09
J6	2011/10/31	0-1	178	±	3	213	±	3	934	±	5	0.36
		1-2	108	±	2	132	±	3	748	±	41	0.49
		2-3	76.3	±	2.5	84.6	±	2.4	686	±	45	0.58
		3-4	20.9	±	2.1	22.1	±	2.3	571	±	39	0.67
		4-5	<2.2			6.2	±	1.7	458	±	35	0.77
		5-6	<2.2			<1.8			466	±	36	0.81
K7	2011/10/29	0-1	42.2	±	1.8	56.2	±	2.0	666	±	17	0.50
		1-2	20.9	±	1.6	18.2	±	1.5	262	±	15	0.85
		2-3	<1.1			<0.9			311	±	14	1.07
		3-4	<1.2			<1.0			120	±	14	1.00
K3	2011/11/1	0-1	59.5	±	3.2	73.6	±	2.7	1064	±	27	0.38
		1-2	<1.6			<1.3			563	±	43	0.74
		2-3	<1.6			<1.3			238	±	43	0.74
J8	2011/10/29	0-1	83.6	±	6.0	97.4	±	5.8	1204	±	24	0.24
		1-2	19.9	±	2.1	29.7	±	2.2	1748	±	35	0.29
		2-3	23.4	±	2.0	26.3	±	1.9	1566	±	36	0.35
		3-4	8.4	±	2.0	15.5	±	1.8	1349	±	45	0.39
		4-5	12.6	±	2.2	15.9	±	2.2	1417	±	51	0.40
		5-6	13.2	±	1.6	15.2	±	1.5	1135	±	19	0.44
		6-7	10.0	±	1.5	12.0	±	1.5	999	±	19	0.43
		7-8	<2.8			<2.3			824	±	19	0.42
		8-9	<2.6			4.6	±	1.4	752	±	19	0.45
		9-10	<2.7			7.5	±	1.3	595	±	19	0.44
K8	2011/10/29	0-1	11.3	±	1.3	15.8	±	2.5	1089	±	34	0.25
		1-2	7.7	±	1.5	11.4	±	1.0	627	±	7	0.48
		2-3	<1.4			<1.2			347	±	16	0.82
		3-4	<1.3			<1.1			136	±	15	0.90
FS1	2011/8/1	0-1	10.3	±	0.8	11.0	±	2.2	961	±	28	0.30
		1-2	2.7	±	1.0	5.8	±	1.5	956	±	26	0.40
		2-3	<1.6			3.0	±	0.9	827	±	19	0.47
		3-4	<1.1			4.0	±	1.1	565	±	15	0.67
		4-5	<0.9			<0.8			404	±	12	0.79
FS5	2011/8/2	0-1	54.1	±	1.4	58.4	±	1.6	1420	±	39	0.26
		1-2	6.6	±	1.1	8.9	±	0.9	ND			0.34
		2-3	3.8	±	0.9	2.3	±	0.7	1175	±	29	0.40
		3-4	3.2	±	0.6	4.1	±	0.5	564	±	27	0.56
		4-5	<1.2			<1.0			223	±	27	0.60

*Activities are decay corrected to sampling date
Uncertainties are given 1-sigma counting errors
ND: No data